Mechanochemical Coupling in Spin-Labeled, Active, Isometric Muscle

Josh E. Baker, Leslie E. W. LaConte, Ingrid Brust-Mascher, and David D. Thomas
Department of Biochemistry, Molecular Biology, and Biophysics, University of Minnesota Medical School, Minneapolis, Minnesota 55455 USA

ABSTRACT Observed effects of inorganic phosphate (P_i) on active isometric muscle may provide the answer to one of the fundamental questions in muscle biophysics: how are the free energies of the chemical species in the myosin-catalyzed ATP hydrolysis (ATPase) reaction coupled to muscle force? Pate and Cooke (1989. *Pflugers Arch.* 414:73–81) showed that active, isometric muscle force varies logarithmically with [P_i]. Here, by simultaneously measuring electron paramagnetic resonance and the force of spin-labeled muscle fibers, we show that, in active, isometric muscle, the fraction of myosin heads in any given biochemical state is independent of both [P_i] and force. These direct observations of mechanochemical coupling in muscle are immediately described by a muscle equation of state containing muscle force as a state variable. These results challenge the conventional assumption mechanochemical coupling is localized to individual myosin heads in muscle.

INTRODUCTION

The primary molecular event responsible for force generation in muscle is thought to be a myosin head (or cross-bridge) rotation that is coupled to the myosin-catalyzed ATP hydrolysis (ATPase) reaction (Reedy et al., 1965; Huxley, 1969; Lymn and Taylor, 1971). In the ATPase reaction, ATP (T) is hydrolyzed on myosin (M) to ADP (D) and inorganic phosphate (P_i) (step 1 in Scheme I). Upon P_i release, myosin binds strongly (stereospecifically) to actin (A) (step 2 in Scheme I; Eisenberg and Hill, 1985) and undergoes a discrete rotation of the myosin light-chain domain (Baker et al., 1998) and an ordering of the myosin catalytic domain (Berger and Thomas, 1994; Thomas et al., 1995). Immediately after ADP release, ATP binds to myosin, dissociating myosin from actin (step 3 in Scheme I; Lymn and Taylor, 1971). In active, isometric muscle, the actin-myosin complex with no nucleotide (A.M) is not significantly populated (Ostap et al., 1995; Dantzig et al., 1992).

To understand mechanochemical coupling in muscle, it is necessary to describe the relationship between muscle force and the chemical potentials of the biochemical species in the myosin ATPase reaction (Scheme I). The chemical potential, μ_i, of a chemical species, *i*, is directly related to its concentration, c_i, as

$$\mu_i = \mu_i^\circ + RT \ln c_i \qquad (1)$$

where $\mu_i°$ is the standard chemical potential, R is the molar gas constant, and T is the temperature (Alberty and Silbey, 1992). Here we have ignored activity coefficients.

For a chemical step that is near equilibrium, the sum of the chemical potentials of the reactants equals the sum of the chemical potentials of the products (Alberty and Silbey, 1992). In active, isometric muscle, these chemical potentials are further balanced by the internal work performed by myosin conformational changes that occur upon actin binding (Baker et al., 1998). In conventional muscle models, it is assumed that this internal work is localized to displacements of elastic elements associated with individual myosin heads (Huxley, 1957; Hill, 1974). Here, we assume nothing about the nature of this internal work; we simply refer to it as the mechanical potential, μ_{mech}. A myosin head rotation is coupled to the actin-binding/phosphate-release step (step 3 in Scheme 1) (Brust-Mascher et al., 1999). If this step is near equilibrium, the free energy equation for this step can be written as $\mu_A + \mu_{M.D.Pi} = \mu_{A.M.D} + \mu_{Pi} + \mu_{mech}$, or in terms of Eq. 1,

$$\Delta G^0 = -RT \ln \frac{[A.M.D][P_i]}{[M.D.P_i][A]} - \mu_{mech} \qquad (2)$$

where $\Delta G° = \mu^\circ_{A.M.D} + \mu^\circ_{Pi} - \mu^\circ_A - \mu^\circ_{M.D.Pi}$ is the standard reaction free energy.

Central to understanding mechanochemical coupling in muscle is explaining how the variables in Eq. 2 ([A.M.D], [M.D.P_i], [P_i], and μ_{mech}) are coupled. In this paper we consider the question, how is a change in [P_i] balanced by changes in [M.D.P_i], [A.M.D], and μ_{mech} in active isometric muscle? By simultaneously measuring electron paramagnetic resonance (EPR) and force of spin-labeled molluscan and skeletal muscle fibers, we show that in active isometric muscle [M.D.P_i] and [A.M.D] are independent of muscle force, F, and [P_i]. In terms of Eq. 2, these results imply that changes in [P_i] can only be coupled to changes in the mechanical potential, μ_{mech}, and so μ_{mech} must vary logarithmically with [P_i] (Eq. 2). Because muscle force, F, also varies logarithmically with [P_i] (Pate and Cooke, 1989; Dantzig et al., 1992), μ_{mech} is a linear function of muscle force, F. Thus, a muscle equation of state containing muscle force as a state variable (Eq. 2, $\mu_{mech} \propto F$) describes direct observations of mechanochemical coupling in muscle. These results challenge the conventional assumption that

Received for publication 30 March 1999 and in final form 21 July 1999.
Address reprint requests to Dr. Josh Baker, Department of Biochemistry, University of Minnesota Medical School, Millard Hall 4-225, 435 Delaware St. NE, Minneapolis, MN 55455. Tel.: 612-626-0113; Fax: 612-624-0632; E-mail: jb@ddt.biochem.umn.edu.

0006-3495/99/11/2657/08 $2.00

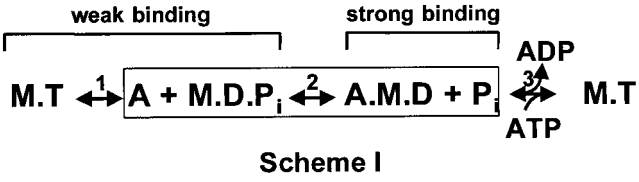

Scheme I

mechanochemical coupling in muscle is localized to individual myosin heads (Hill, 1974).

MATERIALS AND METHODS

Muscle fiber preparation

Skinned rabbit psoas muscle fibers with 4-(2-iodoacetamido)-2,2,6,6-tetramethyl-1-piperidinyloxy spin labels (IASL) covalently attached to Cys^{707} (SH1) in the myosin catalytic domain (IASL-SH1) were prepared as previously described (Ostap et al., 1995). Skinned scallop muscle fibers with 3-(5-fluoro-2,4-dinitroanilino)-2,2,5,5-tetramethyl-1-pyrrolidinyloxy spin labels (FDNASL) covalently attached to Cys^{108} on gizzard regulatory light chains (RLC) functionally exchanged with native RLCs on myosin (FDNASL-RLC) were prepared as previously described (Brust-Mascher et al., 1999).

EPR acquisition

X-band EPR spectra of IASL-SH1 (Ostap et al., 1995) and FDNASL-RLC (Baker et al., 1998) muscle fibers were acquired with a Bruker ESP 300 spectrometer as previously described.

EPR spectra of small IASL-SH1 fiber bundles were acquired using a loop-gap resonator (Hubbel et al., 1987), customized for use with muscle mechanics experiments. Features of this new loop-gap resonator (LGR) design include 1) access to the plate above the resonator block, 2) a resonator block sealed from buffer, and 3) new plates on the top and bottom of the resonator block for mounting fiber mechanics equipment. Muscle fibers were threaded into a fire-polished quartz capillary with an inner diameter of 0.4 mm and an outer diameter of 0.55 mm (Vitro Dynamics, Rockaway, NJ), which was inserted through the resonator.

An EPR spectrum is the EPR signal intensity as a function of magnetic field strength, but to measure transient changes in muscle EPR we measured the EPR signal intensity at a fixed magnetic field position as a function of time. To minimize the effects of EPR baseline drift, we acquired an EPR difference signal as follows. An EPR signal was continuously detected with a Bruker ESP 300 spectrometer and digitized on a PC while the magnetic field was toggled between two field positions every 2.5 s. A C++ program was used to delete data acquired during the signal channel and field controller response period and output the amplitude of the recorded 5-s square wave.

Force measurements

Muscle force, *F*, measurements made during EPR signal acquisitions (Baker et al., 1996) were obtained using a sealed chamber containing a SensoNor Ackers 801 strain gauge (Askjelskapet, Norway). The chamber was made from a 13 × 13 × 16 mm plastic block. The well consisted of an 8-mm hole bored 9 mm into one of the long sides of the block. A second hole (5-mm diameter) was drilled from one of the short sides of the block into the well. A hollow brass cylinder (5-mm outer diameter, 1-mm inner diameter) was inserted into the 5-mm hole, and the strain gauge was mounted inside the brass cylinder, so that the strain gauge extended into the well. Finally, a 1-mm-diameter hole was drilled into the block. The fiber was tied on both ends with surgical thread and pulled into a capillary. The capillary was partially inserted into the 1-mm-well hole, and the surgical thread extending from the capillary was attached to the strain gauge. The other end of the capillary was inserted through the EPR cavity or loop gap resonator, and the thread extending from this end of the capillary was secured with Tygon tubing. The block was attached either to the side plate of the TM_{101} cavity or to the bottom plate of the LGR with four brass screws. The open end of the well was sealed with a plastic cover, and Tygon tubing was attached to a small hole in the cover. Buffer from a reservoir was passed over the fibers by drawing buffer from the well with a peristaltic pump (Ostap et al., 1995). The force and EPR signals were digitized with a PC.

Data analysis

As previously described, the mole fraction, x_i, of myosin heads in state *i* was determined directly from the relative intensity of the corresponding component in the EPR spectrum (Ostap et al., 1995; Baker et al., 1998). In active isometric muscle, we simultaneously measured steady-state muscle force, *F*, and the steady-state mole fraction, x_i, of myosin heads in biochemical state *i* before ($-P_i$) and after ($+P_i$) excess P_i was added. The relative change in muscle force, $\Delta F = [F(+P_i) - F(-P_i)]/F(-P_i)$, and the change in myosin head mole fractions, $\Delta x_i = x_i(+P_i) - x_i(-P_i)$, were then determined. In our analysis, we assume that $[P_i] = 2$ mM in muscle fibers with no added P_i (Cooke and Pate, 1985). As previously observed, scallop muscle does not fully relax when transferred from contraction to relaxation solution (Simmons and Szent-Gyorgyi, 1985). We assume that this resting force is not active force, and we therefore determine the active muscle force, *F*, as the difference between force with Ca^{2+} and force after Ca^{2+} removal.

Buffers

Rigor (no ATP), relaxation (ATP), and contraction buffers (ATP + Ca^{2+}) for IASL-SH1 (Ostap et al., 1995) and FDNASL-RLC (Baker et al., 1998) experiments were prepared as previously described. A stock solution of 50 mM Na_3VO_4 (vanadate) was prepared as described by Barnett and Thomas (1987). When inorganic phosphate or vanadate was included in the contraction buffers, the ionic strength of the contraction buffer was maintained with potassium propionate.

RESULTS

EPR spectra of spin labels that are strongly immobilized and well oriented on myosin in muscle are sensitive to changes in myosin head orientations. EPR of maleimide spin labels that are covalently attached to SH1 in rabbit skeletal muscle (MSL-SH1) is highly sensitive to changes in the myosin catalytic domain orientation (Berger and Thomas, 1994; Thomas et al., 1995). Using EPR of the MSL-SH1 muscle preparation, Zhao et al. (1995) showed that the distribution of myosin catalytic domain orientations is independent of $[P_i]$ and force in active isometric muscle. Based on conventional muscle models, they concluded that a rotation of the myosin catalytic domain is not coupled to P_i release or force generation, and that a rotation of the myosin light-chain domain, therefore, must be coupled to P_i release and force generation. However, we now show that the distribution of myosin light-chain domain orientations is also independent of $[P_i]$ and force in active isometric muscle.

EPR spectra of FDNA spin labels attached to the myosin light-chain domain in scallop muscle (FDNASL-RLC) are highly sensitive to changes in the myosin light-chain domain orientation (Baker et al., 1998). The EPR spectrum of

actin-detached myosin heads (weak-binding states in Scheme I) shows that myosin heads can have one of two distinct orientations, whereas the spectrum of actin-attached myosin heads (strong-binding state in Scheme I) shows that myosin heads have primarily a single LC domain orientation. The EPR spectrum of active isometric muscle is a linear combination of the weak and strong-binding EPR spectral components (Baker et al., 1998).

The steady-state distribution of myosin LC domain orientations in active, isometric muscle is independent of both [P_i] and muscle force

Fig. 1 *a* shows FDNASL-RLC muscle force measurements taken during the acquisition of EPR spectra. The EPR spectra of FDNASL-RLC muscle were acquired with (Fig. 1 *b*, *red*) and without (Fig. 1 *b*, *black*) 50 mM excess P_i after steady-state isometric force was reached. The mole fraction of myosin heads in the A.M.D state was directly determined from the relative intensity of the strong-binding spectral component (Fig. 1 *b*, *inset*). The change in the fraction of myosin heads in the A.M.D state ($\Delta x_{A.M.D}$) and the change in muscle force (ΔF) after 50 mM P_i was added to active, isometric muscle were calculated for each experiment and then averaged over multiple experiments (Table 1). Our data show (Table 1) that a 25-fold increase in [P_i] decreases muscle force by 14%, yet changes the mole fraction of the A.M.D state by less than 1%.

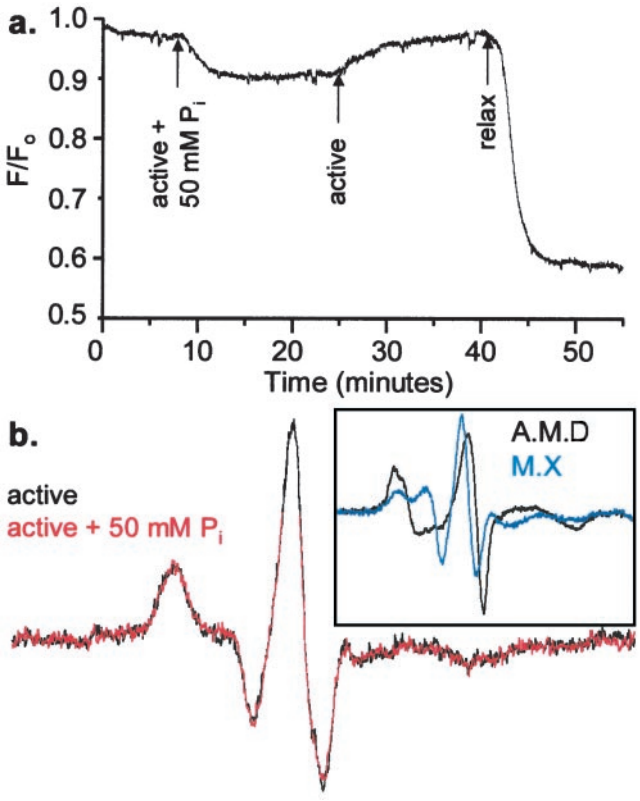

FIGURE 1 Addition of 50 mM P_i to active, isometric FDNASL-RLC scallop muscle. (*a*) Force trace acquired during acquisition of EPR spectra, where F_o is the maximum active, isometric force. (*b*) Overlaid EPR spectra of active isometric FDNASL-RLC muscle acquired during steady state (*black*) with no excess P_i and (*red*) with 50 mM excess P_i. These spectra can be resolved into two spectral components (*inset*): a weakly binding spectral component (M.X = M.T or M.D.P_i) that represents an equal distribution between two LC domain orientations (*ovals*) and a strongly binding spectral component (A.M.D) that represents a single LC domain orientation (Baker et al., 1998).

Similarly, Fig. 2 *a* shows FDNASL-RLC muscle force measurements taken during the acquisition of EPR spectra. The EPR spectra of FDNA-RLC muscle were acquired with (Fig. 2 *b*, *red*) and without (Fig. 2 *b*, *black*) 1 mM vanadate, V_i, a P_i analog (Goodno and Taylor, 1982), after steady-state, active, isometric force was reached. The change in the fraction of myosin heads in the A.M.D state ($\Delta x_{A.M.D}$) and the change in muscle force (ΔF) after 1 mM V_i was added to active, isometric muscle were calculated for each experiment and then averaged over multiple experiments (Table 1). Our data show (Table 1) that the addition of 1 mM V_i decreases muscle force by over 75%, yet changes the mole fraction of the A.M.D state by less than 1% (Table 1).

The above results show that the distribution of myosin head LC domain orientations is independent of both [P_i] and muscle force in active, isometric muscle. Two models can explain this result. In model A, a myosin LC domain rotation is coupled to P_i release and force generation, but phosphate concentrations, [P_i], are coupled to steady-state muscle force, not steady-state myosin concentrations, [A.M.D] and [M.D.P_i] (Eq. 2). This model would suggest that when P_i is added to active, isometric muscle, myosin heads transiently detach from actin at high forces before reattaching to actin at lower forces. In model B, a myosin LC domain rotation is uncoupled from both P_i release and force generation. There is significant experimental evidence for model A. Nevertheless, we further test this model by using muscle EPR to resolve mole fractions of myosin biochemical states rather than mole fractions of myosin orientational states, assuming that there is a difference.

The steady-state distribution of myosin heads among biochemical states is independent of both [P_i] and muscle force in active, isometric muscle

The mobility of weakly immobilized iodoacetamide spin labels (IASL) covalently attached to SH1 in the myosin catalytic domain (IASL-SH1) is affected by local conformational changes near the myosin active site that occur with ATP hydrolysis and P_i release (Ostap et al., 1995). Therefore, EPR spectra of IASL-SH1 can be resolved into spectral components that correspond to the M.T, M.D.P_i, and A.M.D myosin states (Scheme I).

Fig. 3 *a* shows muscle force measurements taken during the acquisition of EPR spectra. The EPR spectra were acquired in active, isometric muscle with (Fig. 3 *b*, *red*) and without (Fig. 3 *b*, *black*) 20 mM excess P_i once steady-state force was reached. These spectra were resolved into the M.T, M.D.P_i, and A.M.D spectral components (Fig. 3 *b*,

TABLE 1 The effects of P_i and V_i on $x_{A.M.D}$ and F in active, isometric, spin-labeled muscle

Preparation	$\Delta x_{A.M.D}$[§]	ΔF[¶]	$\Delta x_{A.M.D}/\Delta F$
FDNASL-RLC + 50 mM P_i^*	0.003 ± 0.01 (n = 6)	−0.14 ± 0.03 (n = 4)	−0.02 ± 0.07[‖]
FDNASL-RLC + 1 mM V_i^*	−0.008 ± 0.009 (n = 9)	−0.76 ± 0.05 (n = 6)	0.01 ± 0.03[‖]
IASL-SH1 + 20 mM $P_I^{*\#}$	0.003 ± 0.01 (n = 5)	−0.40 ± 0.06 (n = 6)	0.02 ± 0.04** (n = 14)

*Experiments on scallop muscle in TM cavity.
#Experiments on rabbit muscle both in TM cavity and LGR.
§From steady-state EPR spectra.
¶From steady-state force measured during EPR experiments.
‖From steady-state experiments (columns $\Delta x_{A.M.D}$ and ΔF).
**Linear correlation between $x_{A.M.D}$ and F from time traces acquired with a LGR. Values given are mean ± standard deviation.

inset). Changes in the mole fractions of the M.T ($\Delta x_{M.T}$ = 0.00 ± 0.01 (n = 5)), M.D.P_i ($\Delta x_{M.D.Pi}$ = 0.00 ± 0.01 (n = 5)), and A.M.D ($\Delta x_{A.M.D}$ = 0.00 ± 0.01, Table 1) states with the addition of 20 mM excess P_i were calculated for each experiment and then averaged over multiple experiments. The results are consistent with the preliminary observations of Ostap (1993). Our data show (Table 1) that the addition of 20 mM P_i decreases muscle force by 40%, yet changes the fraction of myosin heads in the M.T, M.D.P_i, and A.M.D states by less than 1%.

In the above experiments, EPR spectra were acquired from large bundles of 20–100 spin-labeled muscle fibers. To minimize [P_i] gradients across the muscle fiber bundles, we repeated the above IASL-SH1 EPR experiments on bundles of 1–10 IASL-SH1 fibers, using a loop-gap resonator to improve EPR sensitivity to small sample sizes. In these experiments, we monitored with time the difference between EPR signals at two magnetic field positions (*arrows* in Fig. 3 *b*). Like the EPR spectrum, the EPR differ-

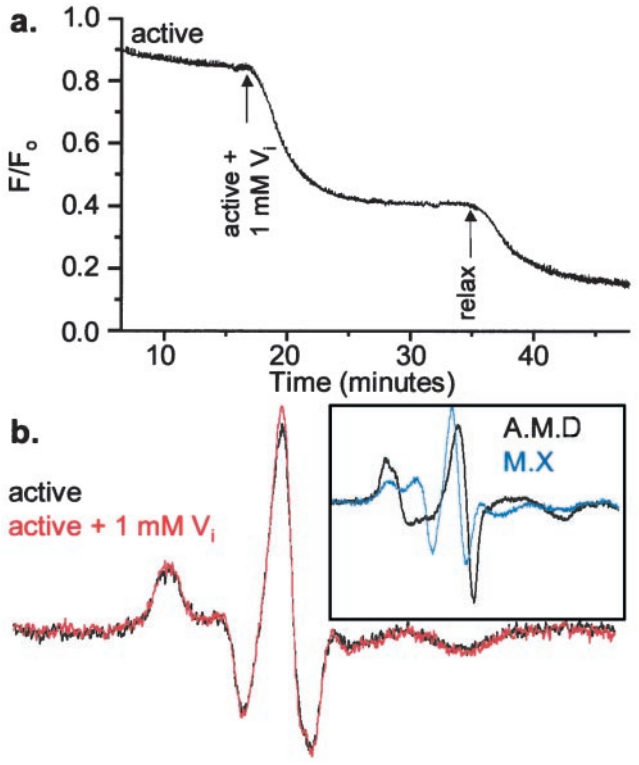

FIGURE 2 Addition of 1 mM V_i to active, isometric FDNASL-RLC scallop muscle. (*a*) Force trace acquired during acquisition of EPR spectra, where F_o is the maximum active, isometric force. (*b*) Overlaid EPR spectra of active isometric FDNASL-RLC muscle acquired during steady state (*black*) with no V_i and (*red*) with 1 mM V_i. Each spectrum is a linear combination of weakly and strongly binding spectral components (*inset*; see Fig. 3).

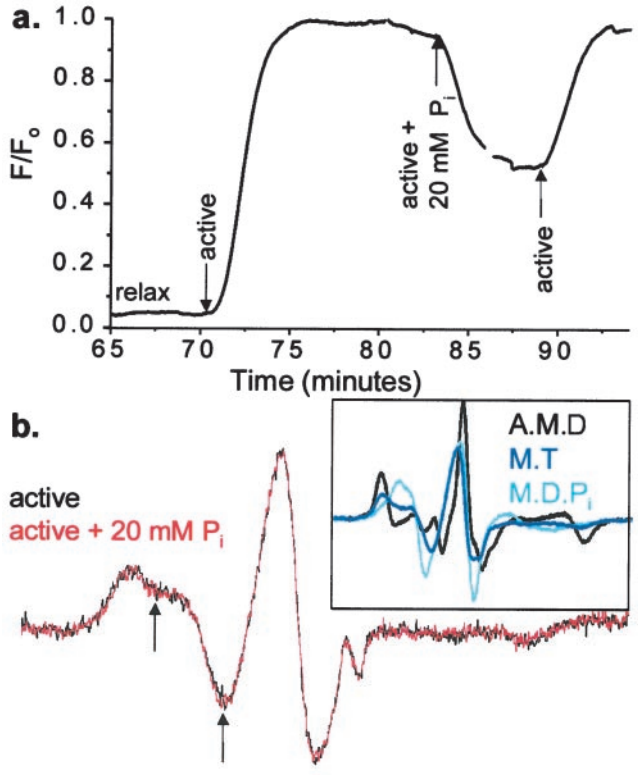

FIGURE 3 Addition of 20 mM P_i to active, isometric IASL-SH1 rabbit muscle. (*a*) Force trace acquired during acquisition of EPR spectra, where F_o is the maximum active, isometric force. (*b*) Overlaid EPR spectra of active isometric IASL-SH1 muscle acquired during steady state (*black*) with no excess P_i and (*red*) with 20 mM excess P_i. Each spectrum is a linear combination of the M.T, M.D.P_i, and A.M.D spectral components (*inset*).

ence signal of IASL-SH1 muscle is a linear combination of the signal in rigor (no ATP, 100% strong-binding) and in relaxation (ATP, 100% weak binding) (Ostap et al., 1995) and varies linearly with the mole fraction of the A.M.D state, $x_{A.M.D}$.

Fig. 4 shows experiments performed on a bundle of ~10 IASL-SH1 fibers, with simultaneously acquired EPR difference signal data and force signal data plotted as functions of time. In Fig. 4, we initially passed relaxation buffer over the muscle fiber(s), which gives the EPR end-point signal corresponding to ~0% of the myosin heads in the A.M.D state ($x_{A.M.D} = 0$). We then passed contraction buffer over the fiber(s), followed by contraction buffer with 20 mM excess P_i. Data tabulated from multiple experiments show that there is no significant correlation between muscle force and the fraction of actin-attached myosin heads in active, isometric muscle ($\Delta x_{A.M.D}/\Delta F$ in Table 1). The EPR difference signal for rigor muscle gives the EPR end-point signal corresponding to nearly all of the myosin heads in the A.M.D state ($x_{A.M.D} = 1$).

The data presented in this paper show that adding P_i to active, isometric muscle has little effect (<1%) on the occupancy of any given biochemical state in the ATPase cycle, whereas it results in a significant decrease (up to 75%) in active, isometric muscle force. These results imply that the *force per actin-attached myosin head decreases with the addition of P_i to active, isometric muscle.* We now quantitatively determine the relationship between $[P_i]$, the distribution of myosin states, and the force per actin-attached myosin head.

DISCUSSION

To understand the coupling of myosin chemical potentials, ligand chemical potentials, and force in muscle (Fig. 5), it is necessary to determine how the fraction of myosin heads in a given biochemical state varies with ligand concentrations and muscle force. The fraction of myosin heads in a given biochemical state in muscle can be accurately determined using EPR of spin-labeled myosin heads. Baker et al. (1998) showed that the mole fraction of myosin heads in the weak- and strong-binding myosin states (Scheme I) can be determined from EPR spectra of FDNASL-RLC scallop muscle fibers. Ostap et al. (1995) showed that the mole fraction of myosin heads in the M.T, M.D.P_i, and A.M.D myosin states (Scheme I) can be determined from EPR spectra of IASL-SH1 rabbit muscle fibers.

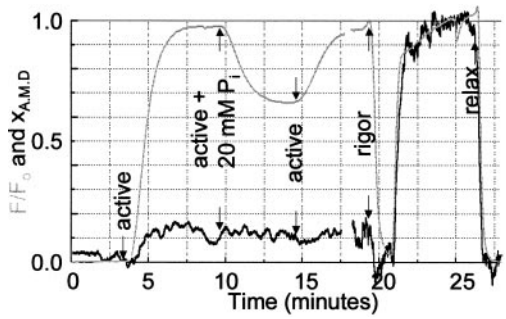

FIGURE 4 Simultaneous measurements of EPR ($x_{A.M.D}$) and relative force (F/F_o) on a bundle of ~10 IASL-SH1 fibers. The force is relative to the maximum active, isometric force, F_o. Both EPR (*black*) and force (*gray*) signals were averaged with a 1.3-min filter from zero to 18 min and a 10-s filter after 18 min. Initially, relaxation buffer (ATP) was flowed over the fiber bundles, followed by contraction buffer (ATP + Ca^{2+}), contraction buffer plus 20 mM P_i, contraction buffer, rigor buffer (no ATP), and relaxation buffer. Immediately after rigor buffer perfusion, both F/F_o and $x_{A.M.D}$ approach 0 before going to 1, suggesting that Ca^{2+} is washed out of the fiber before ATP.

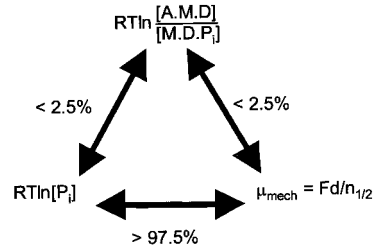

FIGURE 5 The extent of coupling between the variables in Eq. 2: $[P_i]$, $[M.D.P_i]$, [A.M.D], and μ_{mech}. In active isometric muscle, fewer than 2.5% of $[P_i]$ changes are coupled to $[A.M.D]/[M.D.P_i]$ changes. Therefore, more than 97.5% of $[P_i]$ changes are coupled to changes in the mechanical potential, μ_{mech}. The observed logarithmic relationship between muscle force and $[P_i]$ shows that the mechanical potential, μ_{mech}, is proportional to the macroscopic muscle force, F.

In active, isometric FDNASL-RLC scallop muscle, 50 mM excess P_i decreased muscle force by over 10% while changing the mole fraction of myosin heads in the A.M.D state by less than 1% (Fig. 1, Table 1). More dramatically, 1 mM V_i, a P_i analog, decreased active, isometric muscle force by over 70% while changing the fraction of myosin heads in the A.M.D state by less than 1% (Fig. 2, Table 1). Similarly, in active, isometric IASL-SH1 rabbit muscle, a 10-fold increase in $[P_i]$ resulted in a decrease in muscle force of more than 30%, with a change in the mole fractions of the M.T, M.D.P_i, and A.M.D states of less than 1% (Figs. 3 and 4, Table 1). These results imply that, in active, isometric muscle, changes in force and changes in $[P_i]$ are not significantly coupled to changes in [A.M.D], $[M.D.P_i]$, or [M.T]. From Eq. 2, we can calculate the extent of this coupling.

If $[P_i]$ were tightly coupled to [A.M.D] and $[M.D.P_i]$, a 10-fold increase in $[P_i]$ would result in a 10-fold decrease in $[A.M.D]/[M.D.P_i]$ (Eq. 2). This corresponds to a predicted 40% decrease in [A.M.D], because with no added P_i, $[A.M.D]/[M.D.P_i]$ is ~1 (Ostap et al., 1995). However, we observe (Figs. 1–3 and Table 1) that a 10-fold or greater increase in $[P_i]$ results in less than a 1% decrease in $[A.M.D] = x_{A.M.D}[M]_{TOT}$, where $[M]_{TOT}$ is the total concentration of myosin heads in our muscle sample. Therefore, from Eq. 2, less than 2.5% (1/40) of a $[P_i]$ change is coupled to a change in [A.M.D], and assuming [A] is constant, more than 97.5% of a $[P_i]$ change is coupled to a change in the mechanical potential, μ_{mech} (Fig. 5).

In essence, a change in $[P_i]$ is tightly coupled to a change in μ_{mech} (Fig. 5), and thus when $[P_i]$ is changed from an initial P_i concentration, $[P_i]_{initial}$, to a final P_i concentration, $[P_i]_{final}$, the corresponding change in the mechanical potential is $\Delta\mu_{mech} = -RT \ln\{[P_i]_{final}/[P_i]_{initial}\}$ (Eq. 2). Muscle mechanics data of Pate and Cooke (1989) show that in active isometric muscle when $[P_i]$ is changed from $[P_i]_{initial}$ to $[P_i]_{final}$, the corresponding change in muscle force is $\Delta F \propto -RT \ln\{[P_i]_{final}/[P_i]_{initial}\}$. Combining these two experimental results, we get

$$\Delta\mu_{mech} \propto \Delta F.$$

Assuming that in unloaded muscle ($F = 0$) the internal work performed, μ_{mech}, is zero, this equation can be written as

$$\mu_{mech} = Fd/n_{1/2}, \quad (3)$$

where d is a constant with units of distance, and $n_{1/2}$ is a constant equal to the number of moles of myosin heads per cross-sectional area of a muscle half-sarcomere. Substituting Eq. 3 into Eq. 2, we obtain the free-energy equation for the actin-binding step,

$$\Delta G^\circ = -RT \ln \frac{[A.M.D][P_i]}{[M.D.P_i][A]} - \frac{Fd}{n_{1/2}}. \quad (4)$$

Thus the above data immediately imply that myosin, actin, and phosphate chemical potentials are coupled to the macroscopic force, F, of the muscle system (Eq. 4). In active, isometric muscle, we observe that a change in $[P_i]$ results in a change in F without a change in the distribution of myosin states [A.M.D.]/[M.D.Pi] (Fig. 5).

Equations 3 and 4 imply that molecular forces in muscle equilibrate among, not within, myosin heads in muscle, challenging the conventional muscle theory formalized by T. L. Hill. In the Hill formalism, it is assumed that the internal work performed over a biochemical step, μ_{mech}, is $\frac{1}{2}ky^2$, where k is a molecular spring constant and y is a molecular spring displacement that is "not dependent on macroscopic external constraints such as load" (Hill, 1989). Yet we have shown (Eq. 3) that μ_{mech} is a linear function of the external load, F. A related assumption in the Hill formalism is that the "force generated or exerted by cross-bridges on the actin filaments is associated with biochemical states (specifically attached states) and not with transitions or biochemical 'steps.'" In contrast, we have shown that the steady-state force exerted by myosin heads is associated with a biochemical step: the average force per myosin head, $F/n_{1/2}$, like thermodynamic forces in general, is determined by the free energy difference between two states (Eq. 4). Finally, in the Hill formalism, mechanochemical coupling (the relationship between chemical potentials and force) is defined for each actin-attached myosin state by a parabola that describes the myosin head molecular free energy as a function of the myosin head spring displacement, y. This parabola is strictly a molecular free energy function and is independent of the macroscopic muscle force. However, we observe that the chemical potential of the A.M.D state is a function of both the macroscopic muscle force, F, (Eq. 4). T. L. Hill writes, "Ordinary biochemical thermodynamics focuses attention on free energy changes involving substrates, products, ligands, etc. Here... we deal with pseudo-isomeric macromolecular states and free energy levels... This is not a conventional point of view" (Hill, 1989). In contrast our results clearly support the conventional view of biochemical thermodynamics in which free energy is not localized to a single component in the system (e.g., an individual myosin head) but is readily exchanged among all of the components of the system. While our results cannot disprove the unconventional view of the Hill formalism, our data significantly restrict the Hill formalism to a small range of improbable models.

According to the Hill formalism, active, isometric muscle force can only change with a redistribution of myosin heads among biochemical states; yet we observe a large decrease in active, isometric muscle force (75%) with no significant myosin head redistribution (<1%). It may be that a redistribution of myosin heads occurs among multiple actin-attached states that are not distinguished by EPR. However, because large decreases in isometric force are observed with no detectable rotation of either the myosin catalytic domain (Zhao et al., 1995) or the myosin light-chain domain (Figs. 1 and 2), such spectroscopically indistinct myosin states could be separated by no more than a 3° myosin head rotation. Moreover, because we observe a large decrease in force with less than a 1% change in the fraction of weak-binding myosin heads (Figs. 1–4), only a small fraction of myosin heads could be redistributed among such actin-attached states. Thus for the Hill formalism to accord with our data, a 75% decrease in muscle force must be described in terms of a small fraction of myosin heads that rotate less than 3° between two actin-attached myosin states.

The data presented in this paper suggest that the fundamental assumption of the Hill formalism—that force and free energy are localized to myosin heads in muscle—is invalid. Arguments of Tanford and additional experimental data support this conclusion. Tanford has long argued against the Hill formalism in favor of solution thermodynamics. He writes, "The solvent is an intimate participant in all reactions. Chemical potentials were introduced into solution thermodynamics by Gibbs to cope with this problem. Local interactions make it invalid to equate the total free energy of the system with the sum of molar free energies of the components" (Tanford, 1984). Experimentally detected compliance in actin and myosin filaments (Huxley et al., 1994; Wakabayashi et al., 1994) implies that myosin heads can freely exchange mechanical free energy with these filaments and with other myosin heads that interact with these filaments, and so, force is not localized to individual myosin heads in muscle. Moreover, the observed large-amplitude, submicrosecond dynamics of myosin heads and actin filaments in muscle (Thomas et al., 1995) imply that muscle filament structure does not strictly determine the force of a given myosin head in a given state. Such com-

plex, nondeterministic molecular interactions and dynamics are implicitly accounted for in solution thermodynamics (Eq. 4), and must be explicitly accounted for in any molecular model of muscle contraction, by using stochastic methods (Daniel et al., 1998).

Equation 4 suggests a new paradigm for interpreting muscle mechanics data. In conventional muscle models, it is often assumed that the change in myosin head force, F, with muscle length is a constant, $k = dF/dy$; thus a decrease in muscle stiffness is thought to result from a decrease in the number of myosin heads in actin-attached states. However, while muscle stiffness decreases with active, isometric muscle force (Kawai et al., 1987), we have shown that the number of actin-attached myosin heads is independent of active, isometric muscle force. This change in muscle stiffness without a corresponding change in the fraction of actin-attached myosin heads might be explained by nonlinear elasticity or slack in any of the series or parallel elastic elements in active, isometric muscle.

The tight coupling between changes in ligand concentrations and changes in muscle force (Fig. 4) solves a significant but overlooked problem in muscle contraction. W. P. Jencks has argued that for work to be performed at a useful rate by an enzyme, the distribution of enzyme states must be balanced (Jencks, 1980). However, as discussed above, if changes in $[P_i]$ were tightly coupled to changes in $[A.M.D]/[M.D.P_i]$, small variations in ligand concentrations would significantly perturb the balanced distribution of myosin heads between these two states. On the other hand, if changes in ligand chemical potentials are coupled to changes in an external potential, as reported in this paper (Figs. 1–4), a balanced distribution of myosin heads can be maintained and useful work can be performed over a large range of P_i concentrations.

Finally, we discuss our results in the context of a novel model of muscle contraction. The observed tight coupling between $[P_i]$ and isometric force suggests that $RT \ln([A.M.D]/[M.D.P_i])$ (Fig. 5) is the energy available for work, because this would fix $[A.M.D] = [M.D.P_i]$ when active, isometric muscle force is reached, and the energy available for work is zero. In the conventional muscle model, it is assumed that the work performed by a myosin head rotation on actin is localized to elastic elements associated with individual myosin heads. In contrast, our data suggest that the internal work performed by such a rotation is not localized to a single elastic element of the muscle system, and so all we know is that this rotation occurs against an average external force, $F/n_{½}$. Therefore, the proportionality constant, d, that we introduced in Eq. 3 is the average displacement against the average muscle force by myosin head rotations that occur upon actin binding. We have observed that the $M.D.P_i$ to A.M.D transition results in a large and discrete rotation of the myosin light-chain domain in muscle (Baker et al., 1998). This observed rotation can account for a d of $\sim$5 nm.

For decades, it has been assumed that mechanochemical coupling is localized to individual myosin heads in muscle. This is the conventional muscle model, but it is based on unconventional biochemical thermodynamics (Hill, 1989, pp. 92–93) and ignores the fact that macromolecules such as myosin exchange free energy including mechanical free energy with other ligands (Tanford, 1984). In this paper, we have shown that the fraction of myosin heads in any given biochemical state in active, isometric muscle is independent of muscle force and $[P_i]$ (Figs. 1–4). This direct observation of mechanochemical coupling in muscle is not easily explained by the conventional muscle theories. However, by the use of solution thermodynamics, this observation is immediately described by a muscle equation of state (Eq. 4) in which muscle force is a state variable of the muscle system.

We thank N. J. Meyer and E. M. Ostap for their collaboration in experiments related to this work. We thank C. Miller, E. Howard, and R. Bennett for their technical assistance.

This work was supported by grants from the Muscular Dystrophy Association, the National Institutes of Health (AR32961), the Minnesota Supercomputer Institute, and the National Science Foundation.

REFERENCES

Alberty, A, and R. Silbey. 1992. Physical Chemistry. John Wiley and Sons, New York. 133, 144, 210, 211.

Baker, J. E., I. Brust-Mascher, S. Ramachandran, L. E. W. LaConte, and D. D. Thomas. 1998. A large and distinct rotation of the myosin light chain domain occurs upon muscle contraction. *Proc. Natl. Acad. Sci. USA.* 95:2944–2949.

Baker, J. E., N. J. Meyer, and D. D. Thomas. 1996. Simultaneous electron paramagnetic resonance and force of a single spin-labeled muscle fiber: correlating muscle mechanics with structural transitions in the catalytic domain of myosin. *Biophys. J.* 70:A266.

Barnett, V. A., and D. D. Thomas. 1987. Resolution of conformational states of spin-labeled myosin during steady-state ATP hydrolysis. *Biochemistry.* 26:314–323.

Berger, C. L., and D. D. Thomas. 1994. Rotational dynamics of actin-bound intermediates of the myosin ATPase cycle in myofibrils. *Biophys. J.* 67:250–261.

Brust-Mascher, I., L. E. W. LaConte, J. E. Baker, and D. D. Thomas. 1999. Myosin light-chain domain rotates upon muscle activation but not ATP hydrolysis. *Biochem.* in press.

Cooke, R., and E. Pate. 1985. The effects of ADP and phosphate on the contraction of muscle fibers. *Biophys. J.* 48:789–798.

Daniel, T. L., A. C. Trimble, and P. B. Chase. 1998. Compliant realignment of binding sites in muscle: transient behavior and mechanical tuning. *Biophys. J.* 74:1611–1621.

Dantzig, J. A., Y. E. Goldman, N. C. Millar, J. Lacktis, and E. Homsher. 1992. Reversal of the cross-bridge force-generating transition by photogeneration of phosphate in rabbit psoas muscle fibres. *J. Physiol. (Lond.).* 451:247–278.

Eisenberg, E., and T. L. Hill. 1985. Muscle contraction and free energy transduction in biological systems. *Science.* 227:999–1006.

Goodno, C. C., and E. W. Taylor. 1982. Inhibition of actomyosin ATPase by vanadate. *Proc. Natl. Acad. Sci. USA.* 79:21–25.

Hill, T. L. 1974. Theoretical formalism for the sliding filament model of contraction of striated muscle. Part I. *Prog. Biophys. Mol. Biol.* 28: 267–340.

Hill, T. L. 1989. Free Energy Transduction and Biochemical Cycle Kinetics. Springer-Verlag, New York.

Hubbel, W. L., W. Froncisz, and J. S. Hyde. 1987. Continuous and stopped flow EPR spectrometer based on a loop gap resonator. *Rev. Sci. Instrum.* 58:1879–1886.

Huxley, A. F. 1957. Muscle structure and theories of contraction. *Prog. Biophys.* 7:255–317.

Huxley, H. E. 1969. The mechanism of muscular contraction. *Science.* 164:1356–1366.

Huxley, H. E., A. Stewart, H. Sosa, and T. Irving. 1994. X-ray diffraction measurements of the extensibility of actin and myosin filaments in contracting muscle. *Biophys. J.* 67:2411–2421.

Jencks, W. P. 1980. The utilization of binding energy in coupled vectorial processes. *Adv. Enzymol.* 51:75–106.

Kawai, M., K. Guth, K. Winnikes, C. Haist, and J. C. Ruegg. 1987. The effect of inorganic phosphate on the ATP hydrolysis rate and the tension transients in chemically skinned rabbit psoas fibers. *Pflugers Arch. Ges. Physiol.* 408:1–9.

Kittel, C., and H. Kroemer. 1980. Thermal Physics. W. H. Freeman and Co., New York. 122–131.

Lymn, R. W., and E. W. Taylor. 1971. Mechanism of adenosine triphosphate hydrolysis by actomyosin. *Biochemistry.* 10:4617–4624.

Ostap, E. M. 1993. Molecular dynamics and biochemical kinetics of actin and myosin. Ph.D. thesis. University of Minnesota, Minneapolis, MN.

Ostap, E. M., V. A. Barnett, and D. D. Thomas. 1995. Resolution of three structural states of spin-labeled myosin in contracting muscle. *Biophys. J.* 69:177–188.

Pate, E., and R. Cooke. 1989. Addition of phosphate to active muscle fibers probes actomyosin states within the powerstroke. *Pflugers Arch.* 414: 73–81.

Reedy, M. K., K. C. Holmes, and R. T. Tregear. 1965. Induced changes in orientation of the cross-bridges of glycerinated insect flight muscle. *Nature.* 297:1276–1280.

Simmons, R. M., and A. G. Szent-Gyorgyi. 1985. A mechanical study of regulation in the striated adductor muscle of the scallop. *J. Physiol. (Lond.).* 358:47–64.

Tanford, C. 1984. The sarcoplasmic reticulum calcium pump: localization of free energy transfer to discrete steps of the reaction cycle. *FEBS Lett.* 166:1–7.

Thomas, D. D., S. Ramachandran, O. Roopnarine, D. W. Hayden, and E. M. Ostap. 1995. The mechanism of force generation in myosin: a disorder-to-order transition, coupled to internal structural changes. *Biophys. J.* 68:135s–141s.

Wakabayashi, K., Y. Sugimoto, H. Tanaka, Y. Ueno, Y. Takezawa, and Y. Amemiya. 1994. X-ray diffraction evidence for the extensibility of actin and myosin filaments during muscle contraction. *Biophys. J.* 67: 2422–2435.

Zhao, L., E. Pate, A. J. Baker, and R. Cooke. 1995. The myosin catalytic domain does not rotate during the working power stroke. *Biophys. J.* 69:994–999.